IUTAM Symposium on *Critical flow dynamics involving moving/deformable structures with design applications*, June 18-22, 2018, Santorini, Greece

The 3D Transition to Turbulence in a Circular Cylinder Wake by Means of Direct Numerical Simulation

Marianna BRAZA[1], Second author[2]

[1]*Institut de Mécanique des Fluides de Toulouse, Unité Mixte C.N.R.S.-I.N.P.T. 5502, Av. du Prof. Camille Soula, 31400 Toulouse, France*
[2]*Second author affiliation*

Abstract.

The three-dimensional transition to turbulence in the flow around flow around a circular cylinder has been analysed physically by performing direct numerical simulation to solve the system of Navier–Stokes equations. The successive stages of 3D transition, beyond the first bifurcation, have been detected first in the incompressible regime, for a circular cylinder configuration. The generation of streamwise vorticity, organised according to spanwise periodic cells has been associated with the development of large-scale coherent spanwise undulations of the originally rectilinear (nominally 2D) alternating vortex rows. The wavelengths of these undulations have been determined versus Reynolds number. As this parameter increases, a further inherent change of the flow transition is obtained and analysed, the natural vortex dislocations pattern. Beyond this change, the increase of Reynolds number yields an abrupt shortening of the spanwise wavelength and the flow undergoes anothertransition step, whose critical Reynolds number is evaluated by the present DNS approach in association with the Ginzburg–Landau model. Therefore, the linear and nonlinear parts of the flow transition have been quantified by means of the amplitude evolution versus time obtained by the present DNS, in conjunction with the mentioned global oscillator model.

Key words: instability, transition, DNS, bluff-bodies, wings, incompressible flow.

1 Introduction

Concerning (times new roman, 13pt) the flow around a circular cylinder, fascinating phenomena occur in respect to the three-dimensionality of originally 2D vortex structures, as Reynolds number increases. The present study focuses beyond the first bifurcation, that consists of amplification of the von Kármán instability and of formation of the main, alternating vortex rows. Previous studies have reported that this first step to transition is essentially two-dimensional [7, 27], following a Hopf bifurcation, also known as a Poincaré–Andronov bifurcation [33]. The critical Reynolds number (order of 47) had been accurately evaluated by the Stuart–Landau global oscillator model, on the basis of the physical experiment by Provansal et al. [34], as well as by continuation methods using the steady-state approach near the threshold [19]. The DNS approach, combined with a 2D analysis of the Navier–Stokes system, offers the possibility to dissociate those mechanisms having a purely

3D origin from those being essentially 2D, where the ensemble of these mechanisms co-exist and interact non-linearly in the context of the physical experiment. Furthermore, the DNS approach provides the detailed time-history related to the establishment of each physical mechanism, where the time-scales of the initial stages are often rather short during an experimental study for this kind of flows. In the context of flows past bluff bodies, there are still few attempts of direct simulation of the transition to turbulence, whereas this approach has been more widely used in case of rectangular configurations, including among other, boundary layer, jet and channel flows. By performing three-dimensional simulations of the flow past the cylinder in the Reynolds number range (100300) it has been quantified that this flow pattern remains essentially two-dimensional up to Reynolds number of order 180 as shown by Persillon and Braza [28], [30]. etc, etc of transition are analysed in detail, in the present study.

2 3D Transition Features in Incompressible Wakes

The Navier–Stokes equations for an incompressible viscous fluid past a circular cylinder are solved in a general curvilinear coordinates system normalised by the cylinder's diameter D and the uniform upstream velocity. A detailed presentation of these equations and of the numerical method developed can be found [30]. The governing equations are written in general curvilinear coordinates in the (x,y) plan while the z-component (in the spanwise direction) is in Cartesian coordinates, as presented in section 3.2.1. The numerical method is based on the 3D full Navier–Stokes equations for an incompressible fluid. The pressure-velocity formulation is used as well as a predictor-corrector pressure scheme of the same kind as the one reported by Amsden and Harlow [4], extended in the case of an implicit formulation by Braza [8] and [9],Braza et al. [7, 12]. The temporal discretisation is done by adopting the Douglas [13] fractional scheme in an Alternating Direction Implicit formulation. The method is second-order accurate in time and space. Centred differences are used for the space discretisation. The staggered grids by Harlow and Welch [17] are employed for the velocity and pressure variables. The Navier–Stokes equations are transformed in
respect to a non-orthogonal, general curvilinear coordinates system in (x,y) plan, while a Cartesian coordinate z is used for the spanwise direction. This ensures the ability and general character of the present solver to take into account any complex body configuration of constant z section. An H-type grid is used because this kind of grid offers the possibility to introduce more physical boundary conditions on the external boundaries and it avoids branch-cut lines. A zoom of the grid around the obstacle is shown in Fig. 1. An original aspect of the present methodology is the extension of the Douglas alternating directionfractional step scheme, initially conceived for a pure diffusion equation, to the complete set of Navier–Stokes equations. The choice of this scheme, instead of the Peaceman and Rachford [26] Alternating Direction Implicit one, that was chosen in a previous 2D study [7], is made due to the high stability properties offered by the Douglas [13] scheme for the 3D problem. The principles of the numerical
algorithm ICARE are based on the reports by Braza [10, 11]. Another useful element of the present numerical method is the extension in 3D of non-reflecting type outlet

boundary conditions, based on the work by Jin and Braza [20] in two dimensions. The boundary conditions are those specified in Persillon and Braza [30] and are summarised in Fig.2. Concerning the spanwise free edges of the computational domain, periodic boundary conditions are applied. A comparison of Neumann type boundary conditions and of periodic ones in respect to their ability in simulating the development of three-dimensionality and of spanwise undulations has been performed in a number of our studies and proven their equal validity [32]. In a first simulation, Newmann boundary conditionsare employed and allowed to assess the preferential spanwise wavelength formation, selected spontaneously buy the flow system. However, this procedure has needed a very long transient time. Therefore, by taking a spanwise length as a multiple of the simulated one and by using periodic boundary conditions,the transient phase has been considerably shortened. n the following sections the results analyse the way the 3D motion is progressively installed in the flow system. The flow evolution in time and space, with emphasis to the spanwise direction, is studied by performing appropriate signal processing techniques (wavelet analysis and autoregressive modelling). The numerical simulations are carried out for a rather long spanwise length value (12D) and part of the instability analysis concerning global oscillator modelshave been carried out by using a spanwise length of 4.5D. The typical grids are of order (250 * 100 * 80) to (280 * 120 *100). The parallel computers used are the IBM-SP2 of CNUSC (Centre National Universitaire Sud de Calcul) and of Cornell Theory Centre, as well as the CRAY C98 and T3E of the national computing centre IDRIS. In the following, x is the direction along the cylinder's downstream axis, parallel to the free-streem u velocity. y is the vertical direction parallel to v velocity and z is the spanwise direction, parallel to w velocity component.

2.1 Onset of three-dimensionality

The present elliptic flow looses the memory of the initial conditions applied, after a transient phase whose time scale depends on the nature of the initial conditions. After detailed numerical tests in our research group [3, 32], it has been shown that the final, established stage, after the transient one is independent on the initial conditions. Therefore, the choice of the initial fields has been done on the criterion of shortening the transient phase. The initial conditions are those of a 2D established flow with vortex shedding, providing a rectilinear configuration of the alternating vortex rows along the span. A special attention is made to ensure that the alternating vortex shedding is extended over the whole downstream distance, and that the wake expansion rate along x is correct, according to the physical experiment. These features have been achieved by ensuring the three following conditions: (1) A sufficiently refined grid along the whole downstream distance and not only in a limited distance around the obstacle; (2) A sufficiently large computational domain in x and y directions, in order to not confine the flow and to allow the correct wake expansion; (3) Adequate boundary conditions in the downstream outlet boundary, that limit the feedback effects and allow travelling the alternating eddies through this fictitious boundary without confinement (Fig. 3a). Therefore, the proper development of the primary instability, the von Kármán mode, is ensured along the whole computational domain (Figure 3a). This is the fundamental characteristic of this category of flows and a prerequisite to study further on the development of sec-

ondary instabilities along the span. In a number of related studies, the alternating character of the vortex shedding is limited within only one or two diameters downstream the obstacle. After a long transient phase, needing more than 300,000 time steps during which the flow remains 2D, the w velocity component (in the spanwise direction) is progressively developed. In order to shorten this phase, a w velocity weak intensity fluctuation is applied in the inlet section along the span. A white noise of dimensionless intensity 10-4 is chosen. Different runs with different values of this intensity within the range (10-4,10-3) have been checked and ensured leading to the same final established stage. A w velocity component typical evolution is shown in Figure 15a. The amplification of this component follows two distinct stages before saturation, a first exponential growth (linear state) and a second, non-linear one, before reaching saturation, as it is also discussed in Section 2.3. It is found that w velocity component is soon organised according to well distinct cells, (Figure 3b), already in the very early stages of onset of the secondary instability, where the w magnitudes are still very weak. As it is therefore expected from the continuity equation for an incompressible fluid, this pattern is followed by appearance of organisation of streamwise vorticity component x (Figure 3c) along the span, as it is shown at time t=780. The birth of streamwise vorticity x is due to the progressive development of w component as Reynolds number increases, owing to the influence of small perturbations mentioned before. Due to the action of consequent small longitudinal perturbations, the selected mode by the present system provided by the direct simulation is the organisation of the streamwise vorticity pattern on counter-rotating vortices. This is in accordance to the elliptic instability theory. It is recalled that the stability of an elliptical vortex configuration (as one of the von Kármán vortices in this case) to small 3D perturbations provides counter-clockwise longitudinal vorticity filaments with selected wavelengths, that can be assessed by elliptic stability theory considerations [39]. Under the effect of the progressive increase of the streamwise vorticity, the 2D main alternating vortices display a weak regular spanwise undulation. This starting 3D modification of the originally rectilinear alternating vortices is shown in Figure 3d. At higher time values, the streamwise vortices become more intense (Figure 3e) and inception of them occurs between two main alternating eddies in the formation region (Figure 3f). Afterwards, the streamwise vortices are displaced towards the wake's shear layer, in the convection region. Figures 4a-4c show the progressive development of mode A in conjunction with the streamwise vortices formation. The intensity of the spanwise undulation increases from time t=680 to t=740 under the simultaneous effect of streamwise vorticity that is strengthened and forms progressively counter-clockwise 'braid' like structures (see pairs of red and yellow vortices), Figures 4a-4d. The undulation of mode A, that appears as an inherent characteristic of the flow obtained by the direct numerical simulation, is clearly visible on the spanwise evolution ofthe vertical velocity component v, (Fig. 5), that displays a spanwise oscillation according to a regular wavelength. A spectral analysis of these evolutions is performed by means of Fast Fourier Transform Fig. 6, to quantify mode A wavelength. The most predominant spatial mode is found 0.1171, yielding a wavelength value z /R=8.54 (z /D=4.27). This value is found in agreement with the range provided by experimental results, as reported by Persillon and Braza [30]. In the present DNS results, there exist phases of the flow where mode A pattern is less regular (see, for example, the iso-vorticity contours in the time interval (800,840)). This irregularity is associated

and announces a further fundamental modification of the spanwise structure of the main, alternating vortex rows, as it will be analysed in the next section.

2.2 The natural vortex dislocations pattern

The instantaneous iso-vorticity fields z and x are first con...

... frequency variation quantified by the present wavelet analysis.

2.3 The spanwise undulation as reynolds number further increases

t Reynolds number values higher than 220230, the present DNS shows that the spanwise undulation undergoes a substantial decrease of its wavelength and the streamwise vortex filaments become more continuous, linking the formation to the convection region (Fig. 13). They pass from the lower towards the upper shear layers, by materialising well distinct vortex paths. This displacement was found to be discontinuous in the case of mode Aundulation (Figure 3f) [41]. Mode B constitutes an abrupt change in the flow transition [41] and it is worthy to examine whether this bifurcation is hysteretic. We have performed detailed direct simulations up to the established stage, from the upper side of Reynolds number (Re = 340) and descending towards Re = 230. The Strouhal number values according to these simulations are shown in Fig. 14 [3] and indicate that this mode is characterised by hysteresis and corresponds to a values-discontinuity (and not a slope discontinuity). The present direct numerical simulation furnishes in detail the amplitude evolution versus period of the flow properties, as it is shown on Fig. 15a, concerning the w velocity component along the rear axis of the near wake. Based on the amplitude results, it is possible to evaluate the real part of the coefficients of the Ginzburg–Landau global oscillator model:

$$\frac{\partial A}{\partial t} = \sigma_r A - l_r \left|A^3\right| + \mu_r \frac{\partial^2 A}{\partial z^2} \tag{1}$$

...

3 Conclusions

he present study is a continuation of our works in the domain of analysis of 3D transition in flows around bluff bodies. A detailed investigation of successive steps of transition is carried out, as Reynolds and Mach number increase. A special emphasis is devoted to the analysis of natural vortex dislocations in the low Reynolds number range. It has been shown that these structures are a systematic and inherent transition feature, modifying drastically the first 3D step to transition, that consists of the development of a regular spanwise undulation. These transition characteristics are predictable by the fully non-linear approach offered by the direct simulation. The present study has quantified in detail the frequency reduction associated with the formation of this kind of vortex structures, by means of autoregressive signal processing and wavelet analysis of the time-dependent velocity and vorticity signals along the span. spanwise location of the dislocation. This feature is obtained

in the time and frequency domains concerning the predominant amplitude of the fundamental frequency.
The interaction of the vortex dislocations with mode A is shown in the present study as a perturbing effect that modifies the regular spanwise undulation formation. etc, etc after a long time scale, including an order of 20 periods of the vortex shedding is the enhancement of the first subharmonic wavelength of mode A, as the most energetic mode. The successive transition step to dislocations mode undergoes a significant shortening of the spanwise wavelength and a modification on the streamwise vortex filaments, in accordance with the physical experiments concerning mode B. By employing the present DNS results, the supercritical nature of this instability has been shown. This successive step of transition is able to be modelled by the Ginzburg–Landau equation, whose real-part coefficients are evaluated on the basis of the present direct simulation results.

Acknowledgements

This work has been carried out in the research group EMT2 (Ecoulements Monophasiques, Transitionnels et Turbulents) of the Institut de Mécanique des Fluides
de Toulouse. It is based on the collaborative efforts of J. Allain, A. Bouhadji, D. Faghani and H. Persillon in the context of their Ph.D theses and post-doctoral research. Part of this work is carried out on the basis of CPU allocations of the two national computer centres of France CNUSC and IDRIS, as well of the Cornell's Supercomputing centre.

Figures can be put either in the text or at the end of the text, as in the example (11pts) ; **(it is also possible to put two figures in the page's width)**
12 pages maximum, including figures and references

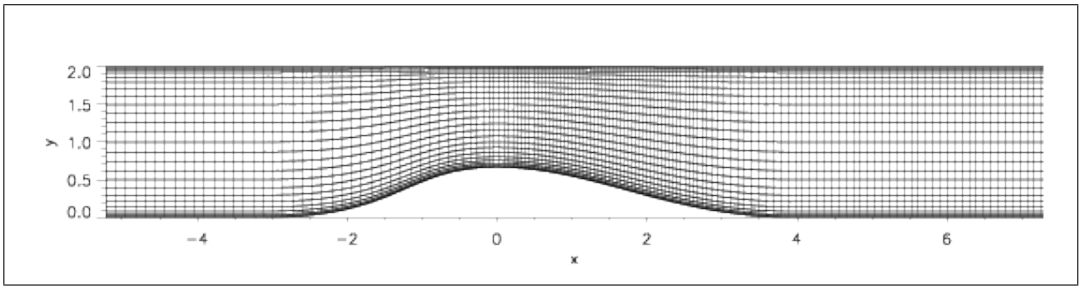

Figure 1: Development of longitudinal vorticity cells between the main eddies in the formation region. (f): Displacement of the longitudinal vortices in the shear layers, in the convection region. Same graduation as in previous figure.